Journal of Biomechanics 71 (2018) 190–198

Contents lists available at ScienceDirect

Journal of Biomechanics

journal homepage: www.elsevier.com/locate/jbiomech
www.JBiomech.com

A visco-hyperelastic constitutive model and its application in bovine tongue tissue

Ali-Akbar Karkhaneh Yousefi [a,*], Mohammad Ali Nazari [a], Pascal Perrier [b], Masoud Shariat Panahi [a], Yohan Payan [c]

[a] School of Mechanical Engineering, College of Engineering, University of Tehran, Tehran, Iran
[b] Univ. Grenoble Alpes, CNRS, Grenoble INP, Gipsa-lab, F38000 Grenoble, France
[c] Univ. Grenoble Alpes, CNRS, Grenoble INP, TIMC-IMAG, F38000 Grenoble, France

ARTICLE INFO

Article history:
Accepted 5 February 2018

Keywords:
Bovine tongue tissue
Visco-hyperelasticity
Passive behavior
Transversely isotropic
Inverse finite element method

ABSTRACT

Material properties of the human tongue tissue have a significant role in understanding its function in speech, respiration, suckling, and swallowing. Tongue as a combination of various muscles is surrounded by the mucous membrane and is a complicated architecture to study. As a first step before the quantitative mechanical characterization of human tongue tissues, the passive biomechanical properties in the superior longitudinal muscle (SLM) and the mucous tissues of a bovine tongue have been measured. Since the rate of loading has a sizeable contribution to the resultant stress of soft tissues, the rate dependent behavior of tongue tissues has been investigated via uniaxial tension tests (UTTs). A method to determine the mechanical properties of transversely isotropic tissues using UTTs and inverse finite element (FE) method has been proposed.

Assuming the strain energy as a general nonlinear relationship with respect to the stretch and the rate of stretch, two visco-hyperelastic constitutive laws (CLs) have been proposed for isotropic and transversely isotropic soft tissues to model their stress-stretch behavior. Both of them have been implemented in ABAQUS explicit through coding a user-defined material subroutine called VUMAT and the experimental stress-stretch points have been well tracked by the results of FE analyses. It has been demonstrated that the proposed laws make a good description of the viscous nature of tongue tissues. Reliability of the proposed models has been compared with similar nonlinear visco-hyperelastic CLs.

1. Introduction

Soft tissues envelope, bind, and connect other parts of the body (Kulkarni et al., 2016). From a mechanical point of view, soft tissues exhibit nonlinear stress-strain behavior, strain rate sensitivity, hysteresis, viscoelastic responses (relaxation and creep), and permanent strains. They have been extensively studied using continuum mechanics and nonlinear elasticity (Humphrey, 2003; Holzapfel and Ogden, 2010).

The tongue is one of the most intriguing human soft tissues because it plays a vital role in respiration, suckling, acquiring and manipulating food, swallowing, and speech. Obviously, not all species use the tongue in the same way, so this organ has evolved to generate deformations into various shapes and mechanisms of movement (Shall, 2012). Especially, human tongue experiences finite strains with high rates during speech production (Gérard et al., 2005; Rastadmehr et al., 2008).

The mammalian tongue is a complex muscular organ which is composed of the mucous membrane, intrinsic and extrinsic muscles (Shall, 2012). Extrinsic muscles originate on structures external to the tongue like bones and insert into the body of the tongue: the genioglossus, the hyoglossus, the styloglossus, the geniohyoid and the palatoglossus. These muscles help the tongue to move in any directions. Intrinsic muscles are fully embedded in the body of the tongue and determine the shape of the tongue: the superior longitudinal, the inferior longitudinal, the verticalis and the transversalis (Gérard et al., 2006).

The muscular tissues have been frequently considered as a network of muscle fibers embedded in an isotropic matrix (Hernández et al., 2011). Skeletal muscles are composed of 70–80% of water so they are usually considered to be incompressible (Takaza et al., 2013). The main course of the fibers determines one of the

* Corresponding author.
E-mail addresses: ali.karkhaneh@ut.ac.ir, ali.karkhaneh@gmail.com (A.-A.K Yousefi), manazari@ut.ac.ir (M.A. Nazari), Pascal.Perrier@grenoble-inp.fr (P. Perrier), mshariatp@ut.ac.ir (M.S. Panahi), Yohan.Payan@univ-grenoble-alpes.fr (Y. Payan).

https://doi.org/10.1016/j.jbiomech.2018.02.008
0021-9290/

directions of material anisotropy and such fibers may be considered as transversely isotropic or orthotropic materials (Martin et al., 1998, 2006). Mechanical behavior of the skeletal muscles can be characterized by their passive and active responses. The passive response can be modeled within the framework of hyperelasticity. The active response which is due to the contractile behavior of the muscle fibers can be represented by some muscle models like Hill-type characteristic behaviors (Nazari, 2011; Martin et al., 1998).

The tongue has been widely investigated experimentally and numerically to describe its actions in the human body (Gérard et al., 2006; Wilhelms-Tricarico, 1995; Dang and Honda, 2002; Vogt et al., 2006; Fujita et al., 2007). The developed FE models intend to improve the understanding of the role of the tongue in linguistics. Kajee et al. (2013) developed a linear elastic FE model of the tongue tissue to better understand its actions in the obstructive sleep apnea syndrome. Using an indentation test, Gérard et al. (2006) proposed an isotropic hyperelastic model of the tongue to investigate its role in speech production. Unfortunately, complex behavior of the tongue tissue has been reduced by much simpler models in previous researches. Due to the lack of experiments, a CL considering the nonlinear nature of tongue tissues, their time dependent response and anisotropic behavior has not been proposed yet.

In higher order mammals, the musculatures of tongues are similar (Gilbert et al., 2006; Shall, 2012). It was therefore decided to focus this paper on bovine tongue tissues since it is still complicated to characterize the biomechanical properties of human tongue tissues. Regarding the distinct ability of the bovine tongue which wraps around the grass and heaves to rip it off, it was hypothesized that both the human and the bovine tongue tissue have similar passive constitutive behavior. This unique function of the bovine tongue is probably due to the fact that the capacity of producing the active force in the muscles of the bovine tongue is more than the human one.

To characterize the mechanical properties of the bovine tongue tissue, the rate dependent and fiber oriented responses of bovine tongue tissue are measured under UTTs. Furthermore, two accurate and reliable visco-hyperelastic CLs are proposed for the passive behavior of isotropic and transversely isotropic soft tissues. Also, in comparison to the well-known CLs, the accuracy of the proposed model in approximating the experimental data is demonstrated.

2. Tests procedure

In order to accurately measure the mechanical properties of the bovine tongue tissue, four freshly slaughtered adult bovine tongues were provided. The sacrifice has been done early morning. Immediately after the sacrifice, the tongue was cut from the larynx and immersed in a saline solution at 4 °C to keep it fresh and prevent its degradation (Hernández et al., 2011; Gras et al., 2012). Due to the complex structure and the direction variation of tongue fibers (Gilbert et al., 2006), cutting an appropriate sample with a fixed fiber direction from each muscle part is difficult in practice. So in the current research, the samples were cut from the mucous membrane and the SLM tissue. The length to width ratio of the samples was at least around 8. These samples underwent a UTT on a Santam STM-1 machine with a 6 kg full-scale load cell. All of the reported data in this paper have been averaged among the measured stress-stretch behavior in different samples dissected from four bovine tongues. Fig. 1 shows the bovine tongue and a corresponding sample during a tensile test.

2.1. Mucous membrane

The mucous membrane has mainly an isotropic structure, so its mechanical properties should be easier to obtain than for tongue muscles. With the aid of a surgical blade, the mucous was separated from the muscles at the tip of the tongue, then some samples were dissected from it. Tests were performed at four different strain rates to measure the elastic and viscoelastic components. Each reported stress-stretch curve for the mucous tissue represents the average measured stress in five samples.

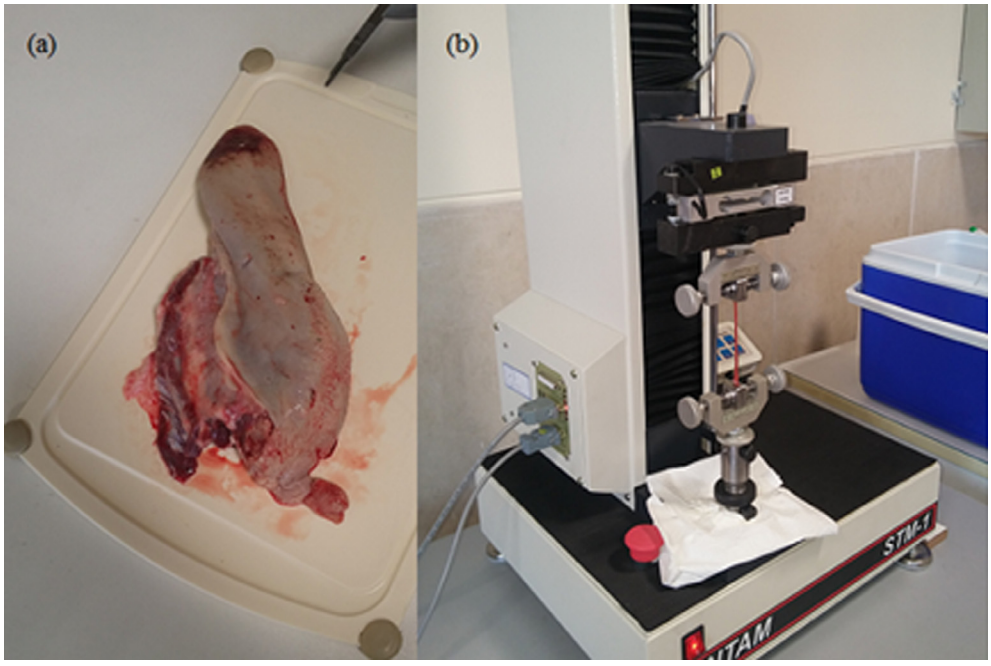

Fig. 1. Bovine tongue (a) and a sample of the superior longitudinal muscle under uniaxial tension test (b).

2.2. Superior longitudinal muscle

The SLM is a thin layer of muscle fibers along the tongue axis located below the mucous membrane and it covers the tongue body. In the bovine tongue tissue, the SLM is combined with the fat tissues in the posterior regions and has a variable thickness in the frontal planes in the anterior regions. So, it is very difficult to dissect a sample from the SLM with 90° and even 45° to the fibers alignment that can be used experimentally. Therefore, in this research, the measurement of the mechanical response of the SLM was limited to the samples aligned with 0°, 20°, and 35° with respect to the fibers' direction.

At the upper surface of the bovine tongue, fibers have a fixed direction along the SLM; our samples were therefore cut from this region. Response of the SLM tissue to the UTTs strongly depends on the angle between the direction of the fibers and the tensile force. Therefore, six samples along the fibers' direction, four samples at 20° to the fibers, and two samples at 35° to the fibers were prepared to measure the average response in the SLM tissue. As for the mucous tissues, tests were performed at different strain rates to quantify the viscous contribution of stress.

3. Constitutive model

A CL has to be chosen to describe the stress-strain relationship of the tissues. Chagnon et al. (2015) reviewed and classified the most popular hyperelastic CLs. Among the many CLs proposed in the literature, those which consider the strain rate as an explicit variable have provided better predictions of viscous behavior especially at higher strain rates (Pioletti et al., 1998; Pioletti and Rakotomanana, 2000; Pioletti, 2006). Furthermore, the domain of validity of other visco-hyperelastic constitutive models, like Fung's quasi-linear viscoelastic law (Fung, 2013) and Holzapfel's model (Holzapfel, 2000), have been restricted to low strain rates (Pioletti et al., 1998; Limbert and Middleton, 2004; Zhurov et al., 2007; Lu et al., 2010).

In this research, the nonlinearity of the stress-strain curves and their dependence on the strain rate are incorporated in the strain energy function through the introduction of powers of strain rates as independent explicit variables.

3.1. Kinematics

Let $\mathbf{X}$ and $\mathbf{x}$ be the position vector of material points in the reference (undeformed) and deformed configuration, respectively. The deformation gradient tensor, $\mathbf{F}$, of any function χ, describing the motion $\mathbf{x} = \chi(\mathbf{X}, t)$, is given by

$$\mathbf{F} = \frac{\partial \mathbf{x}}{\partial \mathbf{X}} \tag{1}$$

which maps any position vector of the reference configuration to the deformed configuration. The right Cauchy-Green strain tensor is given by $\mathbf{C} = \mathbf{F}^{\mathrm{T}}\mathbf{F}$. For three dimensional hyperelastic CLs representing isotropic materials, it is common to use the invariants of a material strain tensor as variables instead of the components of the tensor itself. So, taking $\mathbf{C}$ as this material tensor, its three principal invariants are defined as

$$I_1 = tr(\mathbf{C}), \quad I_2 = \frac{1}{2}[tr(\mathbf{C})^2 - tr(\mathbf{C}^2)], \quad I_3 = \det(\mathbf{C}) = J^2 \tag{2}$$

in which J is the Jacobian and represents the ratio of volume change during the deformation. For materials reinforced with one family of fibers, the principal invariants defined by Eq. (2) are not sufficient to describe the behavior. Hence, for transversely isotropic materials with a preferred fiber direction specified by the unit vector $\mathbf{N}$ in the reference configuration, the structural tensor $\mathbf{A}$ and two additional invariants $I_{4,5}$ are defined as:

$$\mathbf{A} = \mathbf{N} \otimes \mathbf{N} \tag{3a}$$

$$I_4 = tr(\mathbf{CA}), \quad I_5 = tr(\mathbf{C}^2\mathbf{A}) \tag{3b}$$

where $\otimes$ represents the dyadic multiplication of two vectors (Spencer, 1984).

It can be easily shown that the rate of the deformation gradient tensor, $\dot{\mathbf{F}}$, and the velocity gradient tensor, $\mathbf{l}$, are related as:

$$\dot{\mathbf{F}} = \mathbf{lF} \tag{4}$$

So, the rate of $\mathbf{C}$ can be shown to be $\dot{\mathbf{C}} = 2\mathbf{F}^{\mathrm{T}}\mathbf{dF}$ where the tensor $\mathbf{d}$ is the symmetric part of $\mathbf{l}$. As for $\mathbf{C}$, the use of the invariants of $\dot{\mathbf{C}}$ are often preferred to propose CLs for viscoelastic materials. In general, for a transversely isotropic material, 12 invariants $(J_1, J_2, \ldots, J_{12})$ of $\dot{\mathbf{C}}$ have been defined (Boehler, 1987). Among them, J_2 and J_5 are the most popular invariants in the proposed viscoelastic CLs for isotropic and transversely isotropic materials, respectively (Pioletti et al., 1998; Limbert and Middleton, 2004; Zhurov et al., 2007; Lu et al., 2010; Kulkarni et al., 2016; Ahsanizadeh and LePing, 2015):

$$J_2 = \frac{1}{2}tr(\dot{\mathbf{C}}^2), \quad J_5 = \mathbf{N} \cdot \dot{\mathbf{C}}^2\mathbf{N} \tag{5}$$

Their derivatives with respect to the $\dot{\mathbf{C}}$ have been presented by Limbert and Middleton (2004).

3.2. Stress

In hyperelasticity, it is postulated that a scalar valued free energy function exists which is called the Helmholtz free energy function. In thermally independent processes, the rate of Helmholtz free energy function is equivalent to the rate of elastic potential $\psi^e(\mathbf{C}, \mathbf{A})$. In order to include the loading rate effects in the resultant stress, $\dot{\mathbf{C}}$ can be considered as an explicit variable in the stress definition, like $\mathbf{S} = \mathbf{S}(\mathbf{C}, \dot{\mathbf{C}})$, where $\mathbf{S}$ is the second Piola-Kirchhoff stress tensor.

For isothermal process, the thermodynamical principles reduce to the satisfaction of the Clausius-Duhem inequality

$$\left(\mathbf{S} - 2\frac{\partial \psi^e}{\partial \mathbf{C}}\right) : \frac{\dot{\mathbf{C}}}{2} \geqslant 0 \quad \forall \mathbf{C}, \dot{\mathbf{C}} \tag{6}$$

in which : represents the double contraction of two tensors. Without energy dissipation, Pioletti et al. (1998) showed that $\mathbf{S} = \mathbf{S}^e = 2\frac{\partial \psi^e}{\partial \mathbf{C}}$ can be a solution for Eq. (6), where $\mathbf{S}^e$ is the elastic part of stress.

In the existence of dissipation, potential viscous function $\psi^v(\mathbf{C}, \dot{\mathbf{C}}, \mathbf{A})$ was defined as $2\frac{\partial \psi^v}{\partial \dot{\mathbf{C}}} = \mathbf{S} - 2\frac{\partial \psi^e}{\partial \mathbf{C}}$. So, the Clausius-Duhem inequality can be written as

$$\frac{\partial \psi^v}{\partial \dot{\mathbf{C}}} : \dot{\mathbf{C}} \geqslant 0 \quad \forall \dot{\mathbf{C}} \tag{7}$$

which is valid for all continuous, non-negative and convex ψ^v (Pioletti et al., 1998). So, for a viscoelastic material, the stress tensor can be represented by

$$\mathbf{S} = 2\frac{\partial \psi^e}{\partial \mathbf{C}} + 2\frac{\partial \psi^v}{\partial \dot{\mathbf{C}}} = \mathbf{S}^e + \mathbf{S}^v \tag{8}$$

where the first term is the quasi-static part of the response and the second term represents the rate dependent measure of the material response in loading.

3.3. Constitutive laws

In the current research, two CLs for better prediction of the viscoelastic behavior of soft tissues are presented. Inspired by Vogel et al. (2017), these CLs are in the viscous potential part and model the isotropic and transversely isotropic behaviors. In the isotropic case, constitutive models are proposed as:

$$\psi^e = p(J-1) + \frac{c_1}{c_2}\left(e^{c_2(I_1-3)} - 1\right) \tag{9a}$$

$$\psi^v = c_3 J_2 (I_1 - 3)^{c_4} \tag{9b}$$

with the Lagrangean multiplier p and the material parameters (MPs) c_{1-4}, in which all of them must have non-negative values to warrant the convexity condition of ψ^e and ψ^v. In ψ^e, the first term ensures the incompressibility constraint of soft tissues.

In the case of a transversely isotropic material, a particular elastic potential function $\psi^e = \psi^e(I_1, J, I_4)$ and a viscous potential function $\psi^v = \psi^v(J_5)$ are proposed as (for $I_4 > 1$):

$$\psi^e = p(J-1) + c_1(I_1-3)^2 + \frac{c_2}{c_3}(I_4-1)^{c_3} \tag{10a}$$

$$\psi^v = c_4 J_5 (I_4 - 1)^{c_5} \tag{10b}$$

with the MPs c_{1-5}, in which all of them have to be non-negative to warrant the convexity condition. For ψ^e, the second term is added to take into account the contribution of the matrix-fiber ensemble in a transversely isotropic material, and the third term accounts for the fibers' resistance to elongation. In order to reduce the number of MPs, the viscoelastic behavior only considers fibers' resistance to loadings. Similar to term $J_2(I_1-3)^{c_4}$ in Eq. (9b), the term $J_5(I_4-1)^{c_5}$ provides a zero value for ψ^v in the reference configuration and ensures a nonlinear relationship for the stress as a function of the strain and strain rate.

The idea of proposing such potential viscous functions is based on the previous viscoelastic models for long-time behavior (creep and stress relaxation) of soft tissues (Davis and De Vita, 2012, 2014; Peña et al., 2011). In order to improve the accuracy of the quasi-linear viscoelastic (QLV) models, it has been demonstrated that the characteristic time constants and dimensionless coefficients of the Prony series have to be considered as a nonlinear function of strain. So, similar to the long-time responses, the rate dependent (short-time) responses of soft tissues must be strongly dependent on the strain. The use of power c_5 in Eq. (10b) and power c_4 in (9b) ensures the existence of a general nonlinear dependency of stress to strain in the proposed CLs.

For the proposed model in Eq. (9), the elastic and viscoelastic part of $\mathbf{S}$ are given by:

$$\mathbf{S}^e = p\mathbf{C}^{-1} + 2c_1 e^{c_2(I_1-3)}\mathbf{I} \tag{11a}$$

$$\mathbf{S}^v = 2c_3(I_1-3)^{c_4}\dot{\mathbf{C}} \tag{11b}$$

in which $\mathbf{I}$ represents the second order identity tensor. With the use of Eq. (10), the similar relationships for stress can be obtained as:

$$\mathbf{S}^e = p\mathbf{C}^{-1} + 4c_1(I_1-3)\mathbf{I} + 2c_2(I_4-1)^{(c_3-1)}\mathbf{A} \tag{12a}$$

$$\mathbf{S}^v = 2c_4(I_4-1)^{c_5}(\mathbf{N}\otimes\dot{\mathbf{C}}N + \mathbf{N}\dot{\mathbf{C}}\otimes\mathbf{N}). \tag{12b}$$

Fig. 2 represents a fully incompressible sample with fibers along the direction of unit vector $\mathbf{N}$ with zero component out of the E1E2 plane. When this sample is loaded along the E1 direction, $\mathbf{F}$ can be written as (Ogden, 2009):

$$\mathbf{F} = \begin{bmatrix} F_{11} & F_{12} & 0 \\ F_{21} & F_{22} & 0 \\ 0 & 0 & F_{33} \end{bmatrix} \tag{13}$$

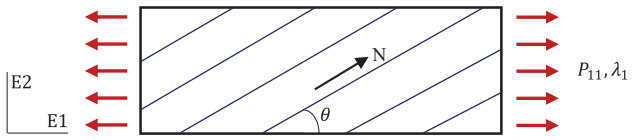

Fig. 2. A transversely isotropic sample under uniaxial tension. Fibers are supposed to be fully laid in the E1E2 plane.

in which the off-diagonal components vanish only for $\theta = 0^\circ$ and $\theta = 90^\circ$; $F_{33} = 1/F_{11}F_{22}$ due to incompressibility assumption. Thus, using the relationship $\mathbf{P} = \mathbf{FS}$, from Eqs. (12) and (13), the components of the nominal stress tensor $\mathbf{P}$ can be obtained as a function of the components of $\mathbf{F}$ and $\dot{\mathbf{F}}$. Also, the traction free boundary conditions in E3 direction leads to an equation, from which the unknown pressure p can be computed. In general, it is not possible to determine all the components of $\mathbf{F}$ for an arbitrary θ. For $\theta \neq 0^\circ$ sample undergoes shear stress in the E1E2 plane. Therefore, there is no explicit relationship between the stress and the controllable parameters of the machine. Thus, an inverse FE method has to be used next to the experimental data points to determine the uncontrollable components of $\mathbf{F}$.

To calculate the time derivative of $\mathbf{F}$ to be used in the FE analysis (FEA), let the deformation gradient tensors at the beginning and at the end of a time increment $\Delta t = t - t_0$ be $\mathbf{F}_{t_0}$ and $\mathbf{F}_t$, respectively. A fully implicit time integration of Eq. (4) yields (Li et al., 2004):

$$\mathbf{F}_t = \exp(\Delta t \mathbf{l}_t)\mathbf{F}_{t_0} \tag{14}$$

in which $\mathbf{l}_t$ represents the velocity gradient tensor at time t. For sufficiently small Δt, Eq. (14) can be approximated by:

$$\mathbf{F}_t \cong (\mathbf{I} + \Delta t \mathbf{l}_t)\mathbf{F}_{t_0} \tag{15}$$

Thus, by use of the calculated velocity gradient tensor from Eq. (15) in Eq. (4), $\dot{\mathbf{F}}$ can be computed.

Also, from Eq. (11) the horizontal component of $\mathbf{P}$, which undergoes a symmetric deformation in E2 and E3 directions, $\lambda_2 = \lambda_1^{-0.5}$, can be obtained as:

$$P_{11}^e = p\lambda_1^{-1} + 2c_1\lambda_1 e^{c_2\left(\lambda_1^2 + 2\lambda_1^{-1} - 3\right)} \tag{16a}$$

$$P_{11}^v = 4c_3\lambda_1^2\dot{\lambda}_1\left(\lambda_1^2 + 2\lambda_1^{-1} - 3\right)^{c_4} \tag{16b}$$

To show the accuracy of the proposed models in predicting the rate dependent behavior, they are compared with one of the most popular transversely isotropic visco-hyperelastic CLs for soft tissues (Limbert and Middleton, 2004; Zhurov et al., 2007; Lu et al., 2010; Kulkarni et al., 2016), originally proposed by Limbert and Middleton (2004):

$$\psi^v = a_1 J_2 (I_1 - 3) + a_2 J_5 (I_4 - 1)^2 \tag{17}$$

a_{1-2} being non-negative MPs. The second term in Eq. (17) is not considered for isotropic materials.

4. Numerical results

In this section, the two CLs proposed to model viscoelastic soft tissues are compared to experimental data collected on different parts of bovine tongue tissue. At first, the elastic MPs have to be determined independently of the viscoelastic MPs by ignoring the potential viscous functions. Then, the viscoelastic MPs can be estimated from one of the tests at a non-zero strain rate. For the mucous tissue, the quasi-static response of the proposed model can be approximated by Eq. (16a). So, parameters $c_{1,2}$ can be obtained by fitting Eq. (16a) to the elastic stress-stretch response via a MATLAB script according to the Levenberg–Marquardt

optimization algorithm. Similarly, the viscous material parameters $c_{3,4}$ and a_1 are estimated by fitting both models to the experimental data points at a strain rate of 1.46%/s. Table 1 compares the results of the parameters estimation for the mucous tissue when our proposed CL is assumed from one side, and with the use of the Limbert's model from the other side. Fig. 3 plots nominal stress versus stretch for the elastic loading and strain rate of 1.46%/s in the mucous tissue. In this figure, the coefficient of determination R^2 as a measurement of goodness of fitting shows that in the both models the MPs are well-defined to follow the experimental points.

Using the estimated MPs, the behavior of the mucous tissue was predicted at different strain rates of 5.46%/s and 6.60%/s. As can be seen from the coefficient of determinations in Fig. 4, our model provides a slightly better prediction than Limbert's model on the viscoelastic behavior of the mucous tissue.

As for the mucous tissue, the proposed CL is evaluated to predict the behavior of the bovine SLM. Eqs. (12a) and (13) are used to define the relationship between **P** and stretch in the muscle. The overall response to the external loading can be approximated by the sum of the resistance to the elongation of the matrix and of the fibers. To compute the contribution of each part, the quasi-static parameters c_{1-3} are calculated from the results of the two quasi-static (elastic) tensile tests with $\theta = 0^\circ$ and $\theta = 20^\circ$. Because **P** in the case of $\theta = 20^\circ$ is not only a function of the controllable parameters of the machine, some complementary tools like an FEA has to be employed to determine the uncontrollable parameters of **F**. So, the use of the FEA besides the results of the uniaxial tension tests leads to a complete determination of portions of the matrix and fibers in the resultant stress.

A first guess of the values of c_{1-3} are approximated from the results of tensile test along the direction of fibers, in which stress-stretch relationship can be simplified to a function of horizontal stretch F_{11} from Eqs. (12a) and (13). The process is similar to elastic MPs estimation of the mucous membrane. Then, the tensile test with $\theta = 20^\circ$ is simulated in ABAQUS explicit by implementing a user-defined material model in subroutine VUMAT. After the analysis, changes of the non-zero components of **F** during the loading time are ready to be used in **P**. Thus, updated values of c_{1-3} can be calculated by minimizing the differences between the measured and predicted stress values at $\theta = 0^\circ$ and $\theta = 20^\circ$ via a MATLAB script according to the Genetic algorithm. The proposed procedure of MPs estimation has to be iterated with the updated parameters to converge to constant values. Fig. 5 shows the required steps to calculate the parameters of a transversely isotropic material via UTTs. The proposed method also can be used for materials with two families of fibers. For this case, the MPs converge to final values with more iterations on UTTs in various angles with respect to fibers' directions.

Fig. 6 shows the elastic response of the proposed model fitted to the experimental data points. The values of c_{1-3} have been determined by fitting the Eq. (12a) to the measured stress at $\theta = 0^\circ$ and $\theta = 20^\circ$. Fig. 6 shows that the proposed CL with the estimated MPs accurately predicts the elastic response of the SLM at $\theta = 35^\circ$. In Table 2 the estimated MPs for this case are provided, in which they have converged to constant values after 5 iterations of the proposed procedure.

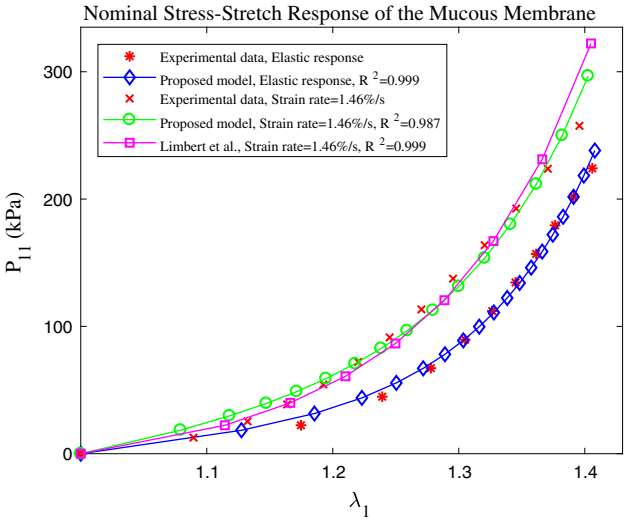

Fig. 3. Behavior of the mucous tissue under uniaxial tensile tests and the fitted constitutive laws.

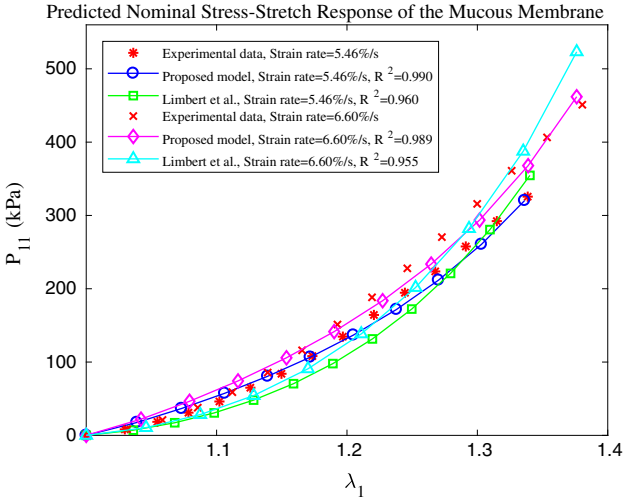

Fig. 4. Comparison of the accuracy of prediction of the rate dependent response of the mucous tissue between the proposed model and Limbert's one.

After determining the elastic MPs, to estimate the viscous behavior of the tissues, MPs $c_{4,5}$ and $a_{1,2}$ are computed by fitting the Eqs. (12b), (13) and (17) to the stress-stretch data points of the tension test along the fibers ($\theta = 0^\circ$) at a strain rate of 1.46%/s. The values of these parameters are reported in Table 2. It is remarkable that the best fitted Limbert's model to the experimental data points does not share any contribution for the fibers in the viscous response of the SLM ($a_2 = 0$), unlike our model in Eq. (10b), in which the viscous part of stress has been restricted to the fibers' effect.

Finally, using these estimated MPs, the accuracy of the proposed model (Eq (10)) is compared with respect to Limbert's

Table 1
Mucous tissue material parameters estimations for the proposed model and for Limbert's model.

	c_1 (kPa)	c_2 (–)	c_3 (kPa)	c_4 (–)	a_1 (kPa)
Proposed model	22.09	4.433	1016	0.606	–
Limbert et al.	22.09	4.433	–	–	1870

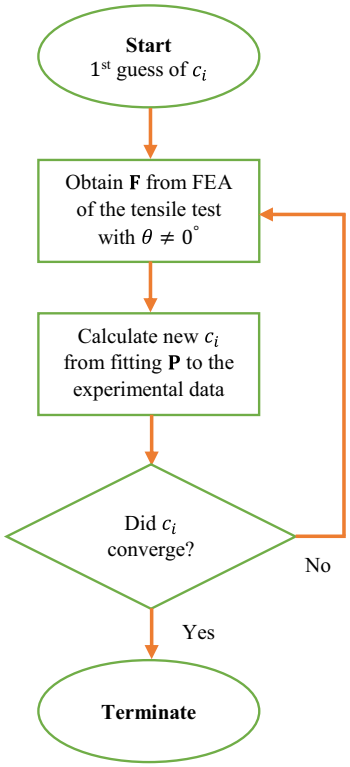

Fig. 5. Flowchart of material parameters estimation procedure of a transversely isotropic material from uniaxial tensile tests.

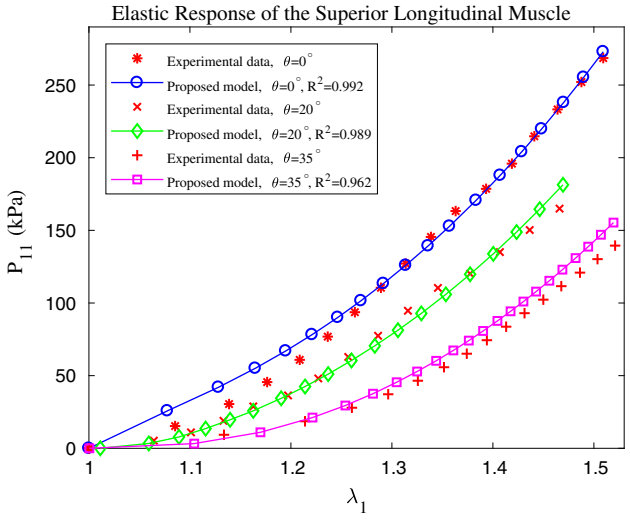

Fig. 6. Elastic response of the superior longitudinal muscle tissue to the uniaxial tension tests in different angles with the fibers' direction. Similarly, the best approximation of the proposed model is depicted.

relationship at a strain rate of 1.65%/s and with $\theta = 20^\circ$ with respect to the fibers. In this case, nominal stress versus stretch is plotted in Fig. 8. Both models have been implemented in the ABAQUS explicit software and nominal stresses at a point far away from the machine grips are plotted in Fig. 8.

It seems that the proposed model predicts significantly more accurately the viscoelastic and the fiber orientation dependent nature of the muscle tissues. This accuracy probably originates from the existence in our model of a more general nonlinear relationship between stress and the stretch and stretch rate. Also, the significant differences of the response predictions in Fig. 8 emphasize

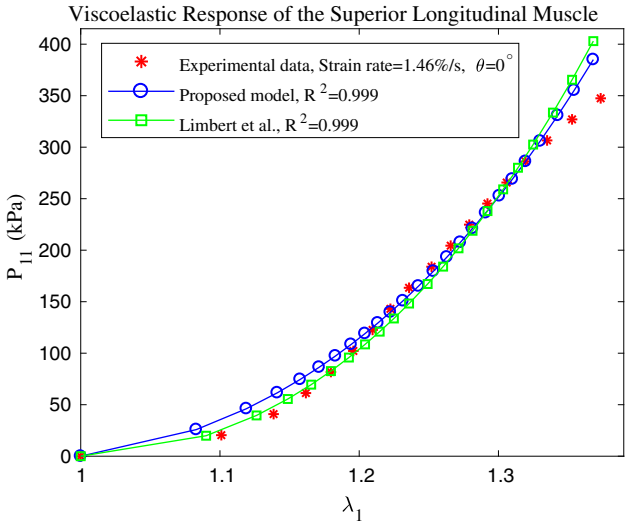

Fig. 7. Fitting the proposed model and Limbert's model to the rate dependent response of the superior longitudinal muscle tissue.

that the viscous response considerably depends more on the fibers than the matrix.

Also, to show that the MPs are uniquely determined and there is not another set of the MPs that can provide an accurate prediction for the SLM, a demonstration has been given in Appendix A.

5. Discussion

During the last two decades, many researchers have studied tongue functions, but very few data were provided as concerns its material properties, in particular, the viscoelastic and anisotropic nature of its tissues. This paper has proposed to address this question by studying the mechanical response of bovine tongue tissues. Appropriate samples from the mucous part of the tongue were dissected and elongated uniaxially at different strain rates. Among the various muscle groups of the tongue, the SLM was chosen because of its ability to provide acceptable macroscopic samples. Such samples were tested at multiple strain rates and in various angles with respect to fibers' direction to determine the stress-stretch responses.

With the aid of inverse FE method, an iteration-based procedure of MPs estimation was proposed for materials with one or two families of fibers. Using the proposed procedure the mechanical properties of these families of materials can be determined via UTTs without any need for biaxial tests. According to this procedure, the material properties of the SLM of bovine tongue tissue did converge to the reported values with only 5 iterations.

Assuming the energy function as a general nonlinear relationship with respect to the stretch and the rate of stretch, two visco-hyperelastic CLs were proposed for the isotropic and transversely isotropic soft tissues, using the invariants of $\mathbf{C}$ and $\dot{\mathbf{C}}$. In addition, the proposed models incorporate the objectivity and convexity constraints for both strain energy function and potential viscous function.

The proposed models were implemented in ABAQUS explicit via a VUMAT subroutine. A good agreement between FEA results and experimental data points validates the estimated MPs of bovine tongue tissue. Compared to a reference visco-hyperelastic CL presented by Limbert, for the isotropic mucous tissue in which the proposed model uses an extra material parameter, a slightly more accurate prediction was obtained. For the transversely isotropic case, in which both the proposed relationship and Limbert's model

Table 2
Material parameters of the bovine superior longitudinal muscle tissue estimated for the proposed model and for Limbert's model.

	c_1 (kPa)	c_2 (kPa)	c_3 (–)	c_4 (kPa)	c_5 (–)	a_1 (kPa)	a_2 (kPa)
Proposed model	38.081	47.863	1.773	1400	1.231	–	–
Limbert et al.	38.081	47.863	1.773	–	–	7079	0

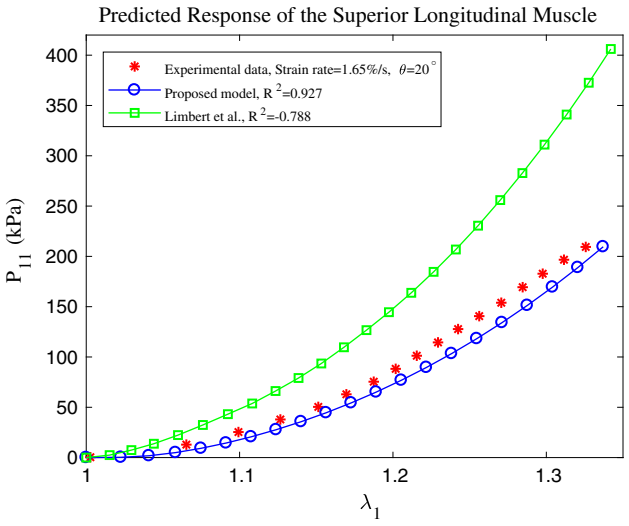

Fig. 8. Comparison of the rate and orientation dependent responses of the superior longitudinal muscle tissue between the proposed model and the one developed by Limbert et al.

use the same number of MPs, our model shows a better agreement with a larger domain of conformity. The proposed models account for large deformation, orientation dependent and viscous behaviors accurately and show their advantage for modeling the behavior of soft tissues.

Acknowledgements

This work has been supported by Center for International Scientific Studies and Collaboration (CISSC) and French Embassy in Tehran in the framework of the project Hubert Curien Gundishapur BIOSTOC.

Conflict of interest

None.

Appendix A. Uniqueness of the estimated material parameters

The proposed CL to describe the passive behavior of the SLM in Eq. (10) has five material parameters c_{1-5}. Each of them represents a specific mechanical behavior of the SLM, c_{1-3} and $c_{4.5}$ in Eq. (10) are considered constituting the elastic and rate dependent responses, respectively. Furthermore, it has to be emphasized that their values are not determined at the same time and after the estimation of the coefficients c_{1-3}, $c_{4.5}$ can be determined. In what follows, it has been demonstrated that the elastic material parameters have been determined uniquely. Then, a similar proof has been provided for the coefficients of Eq. (10b).

To describe the behavior of a transversely isotropic material, it is necessary to consider both the matrix and fibers' effects. Thus, at least two independent material parameters have to be used in a constitutive law. But the sufficiency of only two material parameters to accurately predict the observed behavior depends on the shape of the measured stress-stretch curves in the experiments. According to this point, a 3-parameter model has been chosen to describe the elastic stress-stretch relationship in the SLM, Eq. (10a).

Basically, the possibility of leading to non-unique values of the material parameters in a specific model originates from using some additional material parameters which can be ignored without a significant decrease in the goodness of fitting. In other words, an extra material parameter provides some extra degrees of freedom to the curve which is not necessary for following the experimental data points. In the proposed model in Eq. (10a), c_1 is the only parameter which has been employed to represent the effects of the matrix in the material resistance and can't be ignored. Also,

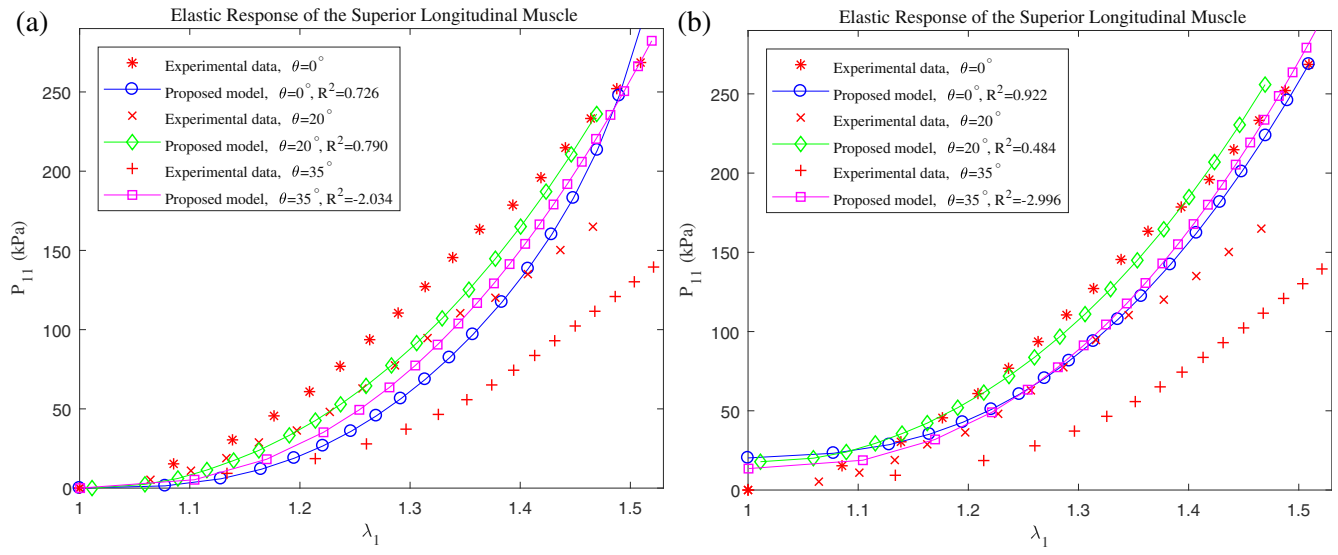

Fig. A1. Best fitted curves to the elastic response of the SLM tissue when c_2 was ignored (a) and when c_3 was ignored (b).

c_2 and c_3 represent the effect of the fibers and perhaps one of them is unnecessary. To examine the question, once c_2 has been disregarded ($c_2 = 1$) in the model and then c_3 has been treated similarly. The best curves fitted to the experimental data points under these conditions, similar to Fig. 6 of the article, are depicted in Fig. A1.

From Fig. A1 it is obvious that a 2-parameter constitutive law roughly predicts the behavior of the SLM. Thus, it seems that at least a 3-parameter model can provide enough degrees of freedom to follow the experimental data points.

In addition, it is supposed to add an extra term like $c_6(I_1 - 3)^3$ to the proposed model in Eq. (10a) and the material parameters have to be tuned in this case. In other words, a 4-parameter constitutive law is chosen for the elastic response of the SLM. For this case, two figures of the best fits like Fig. 6 in the article are depicted in Fig. A2.

As it can be seen from Fig. A2, the figures can go on and on with different values of the material parameters because an extra degree of freedom was included in the model. So, it can be deduced that the three parameters are the minimum required number of material parameters in the proposed model to describe the elastic behavior of the SLM and they converged to the unique values which have been reported in the article.

Similar proofs to show that the rate dependent material parameters in Eq. (10b) have been uniquely determined can be provided here. It is supposed that there is no need for two independent material parameters to predict the rate dependent behavior of the SLM. Thus, the goodness of fitting has to be examined when either c_4 or c_5 is disregarded. Like Fig. 7 in the article, the best fitted curves to the viscoelastic stress-stretch data points at $\theta = 0^\circ$ are given in Fig. A3.

It seems that the fitted curve which is given in Fg. A3(b) accurately follows the experimental data points. But when it was examined to predict the response of the SLM in another direction, it did not result in an accurate prediction compared to the one which has been reported in the article. So, it was decided to add the coefficient c_5 to the proposed model in Eq. (10b) to provide a better description to the soft tissues.

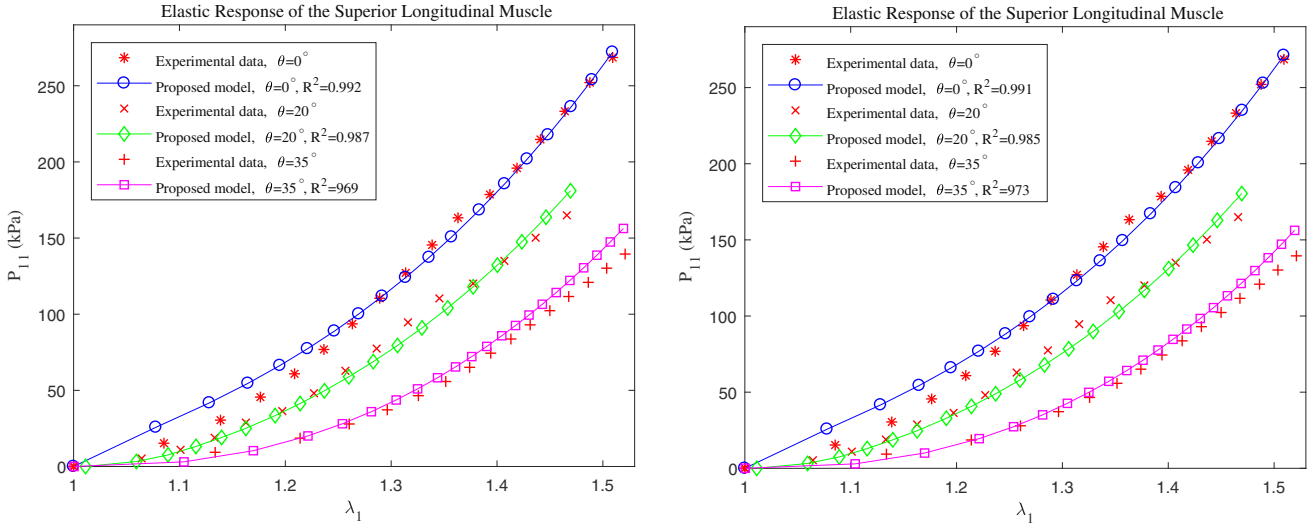

Fig. A2. Best fitted curves to the elastic response of the SLM tissue when an extra term was added to Eq. (10a).

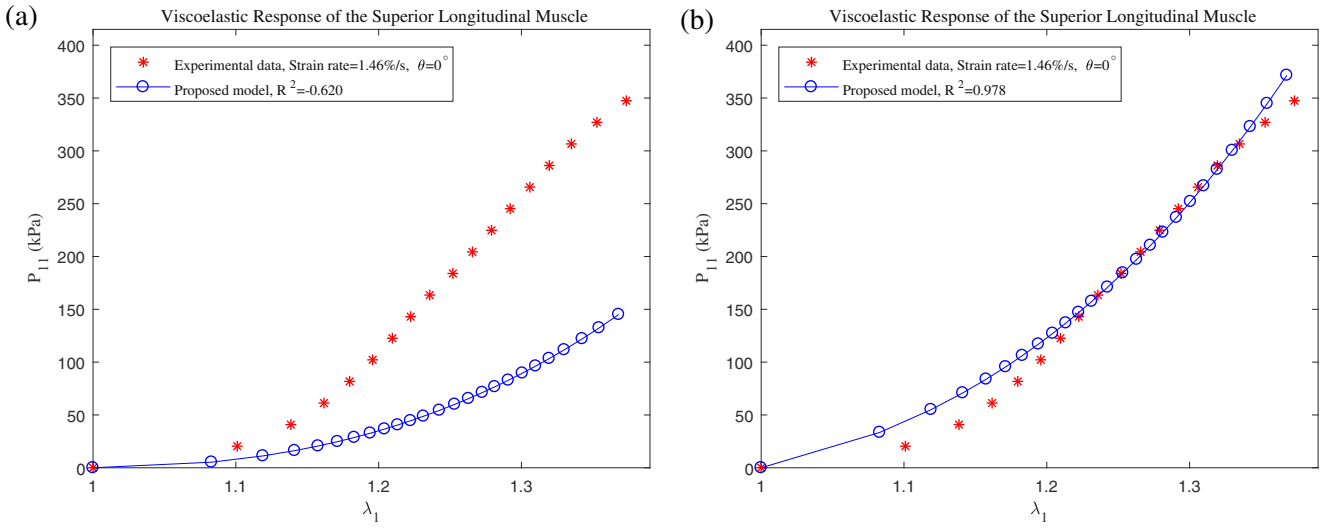

Fig. A3. Best fitted curves to the rate dependent response of the SLM tissue when c_4 was ignored (a) and when c_5 was ignored (b).

Appendix B. Supplementary material

Supplementary data associated with this article can be found, in the online version, at https://doi.org/10.1016/j.jbiomech.2018.02.008.

References

Ahsanizadeh, S., Li, L., 2015. Visco-hyperelastic constitutive modeling of soft tissues based on short and long-term internal variables. Biomed. Eng. Online 14 (1), 29.

Boehler, J.P., 1987. Applications of tensor functions in solid mechanics, vol. 292. J. P. Boehler (Ed.). Springer, New York.

Chagnon, G., Rebouah, M., Favier, D., 2015. Hyperelastic energy densities for soft biological tissues: a review. J. Elast. 120 (2), 129–160.

Dang, J., Honda, K., 2002. Estimation of vocal tract shapes from speech sounds with a physiological articulatory model. J. Phonet. 30 (3), 511–532.

Davis, F.M., De Vita, R., 2012. A nonlinear constitutive model for stress relaxation in ligaments and tendons. Ann. Biomed. Eng. 40 (12), 2541–2550.

Davis, F.M., De Vita, R., 2014. A three-dimensional constitutive model for the stress relaxation of articular ligaments. Biomech. Model. Mechanobiol. 13 (3), 653–663.

Fujita, S., Dang, J., Suzuki, N., Honda, K., 2007. A computational tongue model and its clinical application. Oral Sci. Int. 4 (2), 97–109.

Fung, Y.C., 2013. Biomechanics: Mechanical Properties of Living Tissues. Springer Science & Business Media.

Gérard, J.M., Ohayon, J., Luboz, V., Perrier, P., Payan, Y., 2005. Non-linear elastic properties of the lingual and facial tissues assessed by indentation technique: application to the biomechanics of speech production. Med. Eng. Phys. 27 (10), 884–892.

Gérard, J.M., Perrier, P., Payan, Y., 2006. 3D biomechanical tongue modeling to study speech production. In: Speech Production: Models, Phonetic Processes, and Techniques. Psychology Press, New York, pp. 85–102.

Gilbert, R.J., Wedeen, V.J., Magnusson, L.H., Benner, T., Wang, R., Dai, G., Roche, K.K., 2006. Three-dimensional myoarchitecture of the bovine tongue demonstrated by diffusion spectrum magnetic resonance imaging with tractography. Anat. Rec. Part A: Discov. Mol. Cell. Evol. Biol. 288 (11), 1173–1182.

Gras, L.L., Mitton, D., Viot, P., Laporte, S., 2012. Hyper-elastic properties of the human sternocleidomastoideus muscle in tension. J. Mech. Behav. Biomed. Mater. 15, 131–140.

Hernández, B., Pena, E., Pascual, G., Rodriguez, M., Calvo, B., Doblaré, M., Bellón, J.M., 2011. Mechanical and histological characterization of the abdominal muscle. A previous step to modelling hernia surgery. J. Mech. Behav. Biomed. Mater. 4 (3), 392–404.

Holzapfel, G.A., Ogden, R.W., 2010. Constitutive modelling of arteries. In: Proceedings of the Royal Society of London A: Mathematical, Physical and Engineering Sciences, vol. 466 (No. 2118), The Royal Society, pp. 1551-1597.

Holzapfel, G.A., 2000. Nonlinear Solid Mechanics, vol. 24. Wiley, Chichester.

Humphrey, J.D., 2003. Review paper: Continuum biomechanics of soft biological tissues. In: Proceedings of the Royal Society of London A: Mathematical, Physical and Engineering Sciences, vol. 459 (No. 2029), The Royal Society, pp. 3–46.

Kajee, Y., Pelteret, J.P., Reddy, B.D., 2013. The biomechanics of the human tongue. Int. J. Numer. Meth. Biomed. Eng. 29 (4), 492–514.

Kulkarni, S.G., Gao, X.L., Horner, S.E., Mortlock, R.F., Zheng, J.Q., 2016. A transversely isotropic visco-hyperelastic constitutive model for soft tissues. Math. Mech. Solids 21 (6), 747–770.

Li, S., Beyerlein, I.J., Necker, C.T., Alexander, D.J., Bourke, M., 2004. Heterogeneity of deformation texture in equal channel angular extrusion of copper. Acta Mater. 52 (16), 4859–4875.

Limbert, G., Middleton, J., 2004. A transversely isotropic viscohyperelastic material: application to the modeling of biological soft connective tissues. Int. J. Solids Struct. 41 (15), 4237–4260.

Lu, Y.T., Zhu, H.X., Richmond, S., Middleton, J., 2010. A visco-hyperelastic model for skeletal muscle tissue under high strain rates. J. Biomech. 43 (13), 2629–2632.

Martins, J.A.C., Pires, E.B., Salvado, R., Dinis, P.B., 1998. A numerical model of passive and active behavior of skeletal muscles. Comput. Meth. Appl. Mech. Eng. 151 (3–4), 419–433.

Martins, J.A.C., Pato, M.P.M., Pires, E.B., 2006. A finite element model of skeletal muscles. Virtual Phys. Prototyp. 1 (3), 159–170.

Nazari, M.A., 2011. Biomechanical Face Modeling: Control of Orofacial Gestures for Speech Production (Doctoral dissertation), Université de Grenoble.

Ogden, R.W., 2009. Anisotropy and nonlinear elasticity in arterial wall mechanics. In: Biomechanical Modelling at the Molecular, Cellular and Tissue Levels, Springer, Vienna. pp. 179–258.

Peña, J.A., Martínez, M.A., Peña, E., 2011. A formulation to model the nonlinear viscoelastic properties of the vascular tissue. Acta Mech. 217 (1–2), 63–74.

Pioletti, D.P., Rakotomanana, L.R., Benvenuti, J.F., Leyvraz, P.F., 1998. Viscoelastic constitutive law in large deformations: application to human knee ligaments and tendons. J. Biomech. 31 (8), 753–757.

Pioletti, D.P., Rakotomanana, L.R., 2000. Non-linear viscoelastic laws for soft biological tissues. Eur. J. Mech. A-Solids, 19(LBO-ARTICLE-2000-002), 749–759.

Pioletti, D.P., 2006. Viscoelastic constitutive law based on the time scale of the mechanical phenomena. In: Mechanics of Biological Tissue. Springer, Berlin Heidelberg, pp. 399–404.

Rastadmehr, O., Bressmann, T., Smyth, R., Irish, J.C., 2008. Increased midsagittal tongue velocity as indication of articulatory compensation in patients with lateral partial glossectomies. Head Neck 30 (6), 718–726.

Shall, M.S., 2012. Tongue biomechanics and motor control. In: Craniofacial Muscles. Springer, New York, pp. 229–240.

Spencer, A.J.M. (Ed.), 1984. Continuum Theory of the Mechanics of Fibre-Reinforced Composites. Springer, New York.

Takaza, M., Moerman, K.M., Gindre, J., Lyons, G., Simms, C.K., 2013. The anisotropic mechanical behaviour of passive skeletal muscle tissue subjected to large tensile strain. J. Mech. Behav. Biomed. Mater. 17, 209–220.

Vogel, A., Rakotomanana, L., Pioletti, D.P., 2017. Visco-hyperelastic strain energy function. In: Biomechanics of Living Organs: Hyperelastic Constitutive Laws for Finite Element Modeling. World Bank Publications, pp. 59–78.

Vogt, F., Lloyd, J.E., Buchaillard, S., Perrier, P., Chabanas, M., Payan, Y., Fels, S.S., 2006. Efficient 3D finite element modeling of a muscle-activated tongue. In: International Symposium on Biomedical Simulation. Springer, Berlin, Heidelberg, pp. 19–28.

Wilhelms-Tricarico, R., 1995. Physiological modeling of speech production: methods for modeling soft-tissue articulators. J. Acoust. Soc. Am. 97 (5), 3085–3098.

Zhurov, A.I., Limbert, G., Aeschlimann, D.P., Middleton, J., 2007. A constitutive model for the periodontal ligament as a compressible transversely isotropic visco-hyperelastic tissue. Comput. Meth. Biomech. Biomed. Eng. 10 (3), 223–235.